

# Sphingosine-1-Phosphate Receptor 1 Regulates Cardiac Function by Modulating $\text{Ca}^{2+}$ Sensitivity and $\text{Na}^+/\text{H}^+$ Exchange and Mediates Protection by Ischemic Preconditioning

Petra Keul, PhD;\* Marcel M. G. J. van Borren, MD;\* Alexander Ghanem, MD; Frank Ulrich Müller, MD; Antonius Baartscheer, PhD; Arie O. Verkerk, PhD; Frank Stümpel, PhD; Jan Sebastian Schulte, MD; Nazha Hamdani, PhD; Wolfgang A. Linke, MD; Pieter van Loenen, PhD; Marek Matus, PhD; Wilhelm Schmitz, MD; Jörg Stypmann, MD; Klaus Tiemann, MD; Jan-Hindrik Ravesloot, PhD; Astrid E. Alewijnse, PhD; Sven Hermann, MD; Léon J. A. Spijkers, PhD; Karl-Heinz Hiller, PhD; Deron Herr, PhD; Gerd Heusch, MD; Michael Schäfers, MD; Stephan L. M. Peters, PhD; Jerold Chun, PhD; Bodo Levkau, MD

**Background**—Sphingosine-1-phosphate plays vital roles in cardiomyocyte physiology, myocardial ischemia–reperfusion injury, and ischemic preconditioning. The function of the cardiomyocyte sphingosine-1-phosphate receptor 1 (S1P<sub>1</sub>) in vivo is unknown.

**Methods and Results**—Cardiomyocyte-restricted deletion of S1P<sub>1</sub> in mice (S1P<sub>1</sub><sup>αMHC<sup>Cre</sup></sup>) resulted in progressive cardiomyopathy, compromised response to dobutamine, and premature death. Isolated cardiomyocytes from S1P<sub>1</sub><sup>αMHC<sup>Cre</sup></sup> mice revealed reduced diastolic and systolic  $\text{Ca}^{2+}$  concentrations that were secondary to reduced intracellular  $\text{Na}^+$  and caused by suppressed activity of the sarcolemmal  $\text{Na}^+/\text{H}^+$  exchanger NHE-1 in the absence of S1P<sub>1</sub>. This scenario was successfully reproduced in wild-type cardiomyocytes by pharmacological inhibition of S1P<sub>1</sub> or sphingosine kinases. Furthermore, Sarcomere shortening of S1P<sub>1</sub><sup>αMHC<sup>Cre</sup></sup> cardiomyocytes was intact, but sarcomere relaxation was attenuated and  $\text{Ca}^{2+}$  sensitivity increased, respectively. This went along with reduced phosphorylation of regulatory myofilament proteins such as myosin light chain 2, myosin-binding protein C, and troponin I. In addition, S1P<sub>1</sub> mediated the inhibitory effect of exogenous sphingosine-1-phosphate on  $\beta$ -adrenergic–induced cardiomyocyte contractility by inhibiting the adenylate cyclase. Furthermore, ischemic preconditioning was abolished in S1P<sub>1</sub><sup>αMHC<sup>Cre</sup></sup> mice and was accompanied by defective Akt activation during preconditioning.

**Conclusions**—Tonic S1P<sub>1</sub> signaling by endogenous sphingosine-1-phosphate contributes to intracellular  $\text{Ca}^{2+}$  homeostasis by maintaining basal NHE-1 activity and controls simultaneously myofibril  $\text{Ca}^{2+}$  sensitivity through its inhibitory effect on adenylate cyclase. Cardioprotection by ischemic preconditioning depends on intact S1P<sub>1</sub> signaling. These key findings on S1P<sub>1</sub> functions in cardiac physiology may offer novel therapeutic approaches to cardiac diseases. (*J Am Heart Assoc.* 2016;5:e003393 doi: 10.1161/JAHA.116.003393)

**Key Words:** calcium sensitization • heart failure • ischemia reperfusion injury •  $\text{Na}^+/\text{H}^+$  exchanger • preconditioning • signal transduction • sphingosine • sphingosine-1-phosphate

Sphingosine-1-phosphate (S1P) is a bioactive sphingolipid that exerts major effects in cardiovascular physiology and disease. Plasma S1P levels have been

associated with stable coronary artery disease, myocardial infarction, transient ischemia occurring during percutaneous coronary interventions, and coronary in-stent restenosis.<sup>1–5</sup>

From the Institute for Pathophysiology, Westdeutsches Herz- und Gefäßzentrum, Universitätsklinikum Essen, Essen, Germany (P.K., G.H., B.L.); Heart Failure Research Center (M.M.G.J.v.B., A.B., A.O.V., J.-H.R.) and Department of Pharmacology & Pharmacotherapy (P.v.L., A.E.A., L.J.A.S., S.L.M.P.), AMC, University of Amsterdam, The Netherlands; Department of Cardiology, Universitätsklinikum Bonn, Bonn, Germany (A.G.); Institute for Pharmacology und Toxikology, Münster, Germany (F.U.M., F.S., J.S.S., M.M., W.S.); Department of Cardiovascular Physiology, Ruhr University Bochum, Bochum, Germany (N.H., W.A.L.); Department of Pharmacology and Toxicology, Comenius University, Bratislava, Slovakia (M.M.); Medizinische Klinik und Poliklinik C, Universitätsklinikum Münster, Münster, Germany (J.S., K.T.); European Institute for Molecular Imaging, Münster, Germany (S.H., M.S.); MRB Forschungszentrum Magnet-Resonanz-Bayern e.V., Würzburg, Germany (K.-H.H.); Department of Molecular Biology, Scripps Research Institute, La Jolla, CA (D.H., J.C.).

Accompanying Data S1, Table S1 and Figures S1, S2 are available at <http://jaha.ahajournals.org/content/5/5/e003393/DC1/embed/inline-supplementary-material-1.pdf>

\*Dr Keul and Dr van Borren contributed equally to this work.

**Correspondence to:** Bodo Levkau, MD, Institute for Pathophysiology, University Hospital Essen, Hufelandstrasse 55, 45122 Essen, Germany. E-mail: bodo.levkau@uni-due.de

Received February 12, 2016; accepted March 23, 2016.

© 2016 The Authors. Published on behalf of the American Heart Association, Inc., by Wiley Blackwell. This is an open access article under the terms of the Creative Commons Attribution-NonCommercial License, which permits use, distribution and reproduction in any medium, provided the original work is properly cited and is not used for commercial purposes.

S1P is an integral constituent of high-density lipoproteins and has been demonstrated to causally contribute to several of their beneficial effects.<sup>6,7</sup> Recently, we have shown that diminished S1P content in HDL from patients with coronary artery disease is a cause of HDL dysfunction and that raising HDL-S1P therapeutically restored HDL function.<sup>7</sup>

Mechanistically, S1P can act as an intracellular signaling molecule and as an extracellular ligand for 5 G-protein-coupled receptors. Three are expressed in the heart (S1P<sub>1</sub>, S1P<sub>2</sub>, and S1P<sub>3</sub>) and were shown to mediate the effects of S1P on different aspects of cardiomyocyte biology.<sup>8–10</sup> In experimental myocardial ischemia–reperfusion models, S1P generated endogenously by cardiac sphingosine kinases or administered exogenously prior to ischemia protects against reperfusion injury, whereas endogenous S1P mediates the cardioprotective effect of ischemic pre- and postconditioning.<sup>8,10,11</sup> Exogenous S1P has been shown to protect through nitric oxide produced following activation of the endothelial S1P<sub>3</sub> receptor,<sup>12</sup> whereas endogenous S1P required Akt activation by both S1P<sub>2</sub> and S1P<sub>3</sub> for efficient cardioprotection.<sup>13</sup> Mice deficient for S1P<sub>2</sub> or S1P<sub>3</sub> have no obvious cardiac phenotype except for the resistance of S1P<sub>3</sub><sup>−/−</sup> mice to the bradycardic effect of the S1P analog fingolimod (Gilenya; Novartis).<sup>14</sup> The S1P receptor responsible for S1P-mediated preconditioning had not been identified prior to our study. In humans, S1P<sub>1</sub> gene polymorphisms have been associated with coronary artery disease and stroke,<sup>15,16</sup> but addressing its physiological role in the heart in vivo has been hampered by the embryonic lethality of global S1P<sub>1</sub> knockout mice.

In this study, we have examined the role of S1P<sub>1</sub> in normal and pathophysiological cardiac function by generating mice with a cardiomyocyte-specific deletion. We provided evidence that S1P<sub>1</sub> is indispensable for normal cardiac function, ion homeostasis, activity of the Na<sup>+</sup>/H<sup>+</sup> exchanger NHE-1, and myofibrillar Ca<sup>2+</sup> sensitivity. Furthermore, we addressed the role of S1P<sub>1</sub> in myocardial ischemia–reperfusion injury and ischemic preconditioning (IP).

## Methods

### Mice

Mice homozygous for a floxed S1P<sub>1</sub> allele<sup>17</sup> were crossed with C57Bl/6J mice heterozygous for the Cre recombinase under the control of the  $\alpha$ -myosin heavy chain ( $\alpha$ MHCCre)<sup>18</sup> to obtain S1P<sub>1</sub> <sup>$\alpha$ MHCCre</sup> mice and littermate controls (S1P<sub>1</sub><sup>fl<sup>ox</sup>/fl<sup>ox</sup></sup>). All procedures followed were in accordance with institutional guidelines.

## Imaging, Echocardiography, and In Vivo Hemodynamic Measurements

Magnetic resonance imaging was performed using a 7-T Bruker NMR spectrometer and <sup>18</sup>F-fluorodeoxyglucose positron emission tomography on a high-resolution small-animal camera (quadHIDAC; Oxford Positron), respectively. High-resolution echocardiography with quantitative 3-dimensional assessment of cardiac function was performed on an ultrasound device with frame rates up to 280 Hz (Philips Medical Systems). Left ventricular (LV) catheterization was performed in closed-chest anesthetized mice, as described previously,<sup>19</sup> with dobutamine administered via the cannulated left jugular vein accompanied by measurements of heart rate, maximal LV pressure, and the first derivative of LV pressure.

## Cardiomyocyte Diameter, Fibrosis, Real-Time Polymerase Chain Reaction, and Western Blotting

The mean cardiomyocyte diameter was measured in 100 cardiomyocytes with longitudinally cut nuclei on periodic acid–Schiff–stained sections and interstitial fibrosis assessed on picrosirius red–stained sections with an image analysis program (KS 300; Zeiss). For gene expression, total RNA was isolated from the left ventricle, cDNA was synthesized using the Revert Aid First Strand cDNA Synthesis Kit (Qiagen), and real-time polymerase chain reaction was performed on a Bio-Rad CFX96 system using iQ SYBR Green. Relative gene expression was calculated by the 2<sup>− $\Delta\Delta$ CT</sup> method and normalized to GAPDH. For Western blotting, myocardial tissue was homogenized in RIPA buffer, run on SDS-PAGE, transferred to nitrocellulose membranes, and blotted with antibodies to phospholamban, which was phosphorylated at serine 16 and threonine 17, respectively, sarcoplasmic reticulum Ca<sup>2+</sup> ATPase 2a, junctin, and calsequestrin (for normalization). The electrochemiluminescence signal was quantified by a Bio-Rad ChemiDoc MP Imaging System. The phosphorylation level of cardiac myosin light chain 2, troponin I, and myosin-binding protein C was determined using the Pro-Q Diamond/Sypro Ruby staining kit (Molecular Probes), as described.<sup>20</sup> Briefly, proteins on gels were stained for 1 hour with Pro-Q Diamond to determine phosphoprotein expression and overnight with Sypro Ruby to measure total protein content. Signals were visualized using the LAS-4000 Image Reader (Fuji Science Imaging Systems) and analyzed using the manufacturer's Multi Gauge version 3.2 software. Phosphorylation levels of myofilament proteins in knockout hearts were expressed relative to those of controls.

## Functional Characterization of Single Cardiomyocytes

Detailed methods are provided in Data S1. LV myocytes were isolated by enzymatic dissociation. Cell size and membrane capacitance of the isolated cardiomyocytes were similar in all genotypes.

### Action potential recordings

Action potentials (APs) were recorded using the perforated patch-clamp technique using an Axopatch 200B amplifier (Molecular Devices). APs were filtered and digitized at 10 and 40 kHz, respectively. APs were elicited at 1 to 10 Hz by 3-ms,  $\approx 1.2 \times$  threshold current pulses through the patch pipette. Resting membrane potential; maximal AP amplitude; maximal upstroke velocity; AP duration at 20%, 50%, and 90% repolarization; and plateau amplitude were analyzed and averaged from 10 consecutive APs.

### Intracellular concentration measurements

Intracellular concentrations of Ca<sup>2+</sup><sub>i</sub>, Na<sup>+</sup><sub>i</sub>, and pH<sub>i</sub> (Ca<sup>2+</sup><sub>i</sub>, Na<sup>+</sup><sub>i</sub>, and pH<sub>i</sub>, respectively) were measured in indo-1, SBFI, and SNARF-1–loaded myocytes preincubated in HEPES-buffered solutions containing 10  $\mu$ mol/L SBFI-AM or 5  $\mu$ mol/L indo-1-AM or 10  $\mu$ mol/L SNARF-1-AM and 0.01% pluronic. Incubation durations were 10, 30 and 120 minutes. Fluorescence of all indicators was measured in dual-wavelength emission mode at 405/505, 410/590, and 580/640 nm. Fluorescence signals were corrected for background recorded from probe-free myocytes and calibrated to obtain maximum and minimum ratio values of the emitted wavelengths and the constants  $\beta$  and  $k_d$ . Na<sup>+</sup><sub>i</sub> was averaged over the entire cardiac cycle. Cytosolic free Ca<sup>2+</sup><sub>i</sub> was obtained by correction of measured overall cellular fluorescence signals for contributions of mitochondrially compartmentalized indo-1. pH<sub>i</sub> was determined from calibration curves obtained with nigericin, and NHE-1–dependent proton flux was calculated from the rate of recovery of pH<sub>i</sub> following acid loading. The sarcoplasmic reticulum Ca<sup>2+</sup> content of cells was studied by 20 mmol/L caffeine application.

### Sarcomere length shortening

Sarcomere length (SL) was measured using a fast Fourier transform algorithm of the video image (200 frames per second) of the contracting myocytes (IonOptix).

### cAMP measurements

The LANCE cAMP kit (PerkinElmer) was used to determine cAMP concentrations using a Victor plate reader (Wallac; PerkinElmer). All experiments were performed in the presence of 0.05% bovine serum albumin and 500  $\mu$ mol/L of isobutylmethylxanthine. Force measurements at different Ca<sup>2+</sup>

concentrations were performed on single demembrated cardiomyocytes, as described previously.<sup>20</sup> Briefly, isolated cells were bathed in relaxing solution (in mmol/L: free Mg 1, KCl 100, EGTA 2, Mg-ATP 4, and imidazole 10; pH 7.0) under an inverted microscope (Zeiss Axiovert 135) and attached with silicone adhesive between a force transducer and a piezoelectric motor as part of a permeabilized myocyte test system (1600A, with force transducer 403A; Aurora Scientific). The myocyte was adjusted to 2.2- $\mu$ m SL and exposed to a series of solutions with different pCa values ranging from 9.0 (relaxing) to 4.5 (maximal activation) to obtain the force–pCa relation (pCa =  $-\log$  of [Ca<sup>2+</sup>]). Force values were calculated relative to the maximal force at pCa 4.5. Mean values on relative force–pCa diagrams were fit with the Hill equation. On the sigmoidal Hill curve, the pCa at 50% of maximum developed force is the Ca<sup>2+</sup> sensitivity of the contractile apparatus.

### Ischemia–Reperfusion Injury and IP

Ischemia–reperfusion injury and IP were performed, as described.<sup>21</sup> In brief, mice of either sex were anesthetized with pentobarbital (80 mg/kg IP) and subjected to 30 minutes of occlusion of the left anterior descending coronary artery and 120 minutes of reperfusion without and with prior IP by 1 cycle of 5 minutes of occlusion of the left anterior descending coronary artery and 10 minutes of reperfusion. At the end of the experiment, the coronary artery was reoccluded, and Evans blue was injected intravenously to delineate the area at risk. After euthanizing the mice by KCl infusion, hearts were excised and cut into 4 to 5 transverse slices, and the infarct size was quantified by triphenyl tetrazolium chloride staining.

### Statistical Analysis

Overall survival curves were estimated using the Kaplan–Meier method, and differences between genotypes were compared by the log-rank test. The Wilcoxon test was used in all experiments with small to moderate sample sizes (<10). ANOVA followed by a Bonferroni post hoc test was used to test for significant differences among groups. For the invasive hemodynamic measurements (Figure 2C), 2-way repeated-measures ANOVA was used, and the indicated significant differences are from the omnibus test. Average data are presented as mean  $\pm$  SEM. Values of  $P < 0.05$  were considered statistically significant.

## Results

### Impaired Cardiac Function in Mice Carrying a Deletion of S1P<sub>1</sub> in Cardiomyocytes

In the murine heart, S1P<sub>1</sub> is the most abundantly expressed S1P receptor (Figure 1A). To address its function in vivo, we

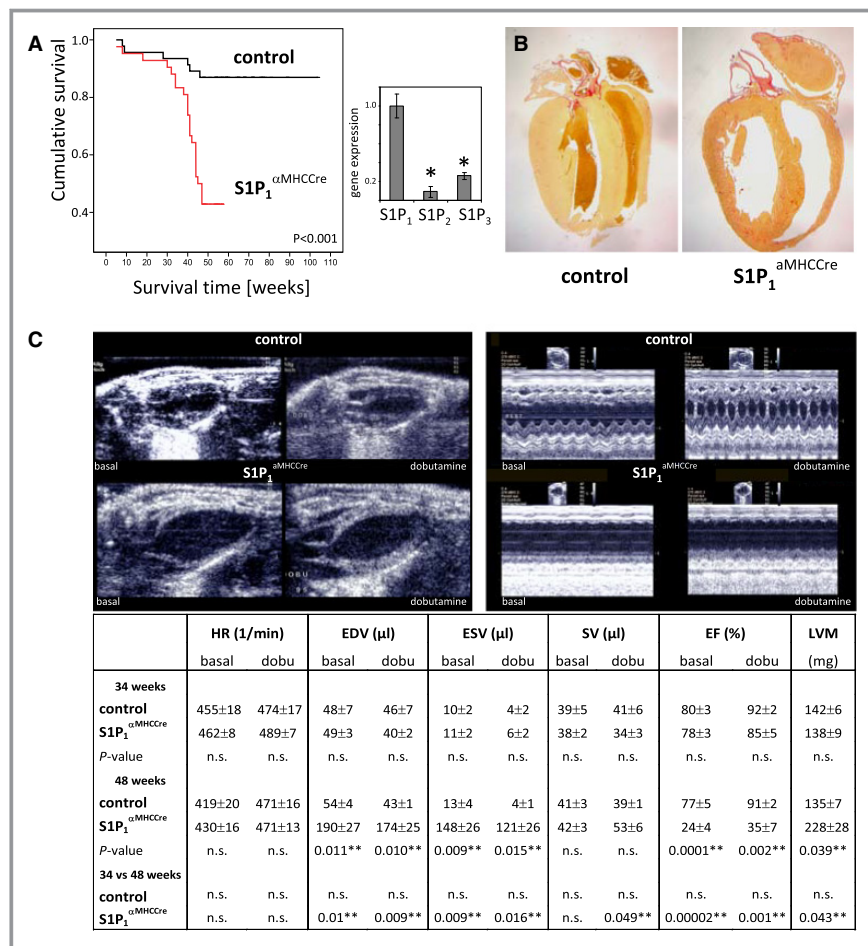


**Figure 1.** Impaired cardiac function of S1P<sub>1</sub><sup>αMHCcre</sup> mice. **A**, Kaplan–Meier survival curves for S1P<sub>1</sub><sup>αMHCcre</sup> mice (n=41) and controls (S1P<sub>1</sub><sup>flox/flox</sup>; n=45). Figure at right shows S1P receptor gene expression in the normal adult mouse heart (C57Bl6) expressed relative to S1P<sub>1</sub>. \*Statistical significance of S1P<sub>1</sub> (n=7, P<0.05). **B**, Representative heart pathology of an S1P<sub>1</sub><sup>αMHCcre</sup> mouse aged 45 weeks and a littermate control. **C**, Representative echocardiography of an S1P<sub>1</sub><sup>αMHCcre</sup> mouse aged 45 weeks and its littermate control under basal conditions and after stimulation with dobutamine. The table shows quantitative assessment of cardiac function under basal conditions (basal) and after intravenous stimulation with low-dose (10 μg/kg per minute) dobutamine by echocardiography in control and S1P<sub>1</sub><sup>αMHCcre</sup> mice at 34 weeks (n=5 and n=7, respectively) and 48 weeks (n=5 and n=6, respectively). **D**, Cardiac magnetic resonance imaging (representative end-systolic and end-diastolic images) and quantification of cardiac function in S1P<sub>1</sub><sup>αMHCcre</sup> mice aged 48 weeks and control mice (n=5 each; \*P<0.05 vs control). **E**, Representative <sup>18</sup>F-fluorodeoxyglucose positron emission tomography images (whole body, cardiac short and long axes) of an S1P<sub>1</sub><sup>αMHCcre</sup> and control mouse aged 31 and 48 weeks. Dobu indicates dobutamine; EDV, end-diastolic volume; EF, ejection fraction; ESV, end-systolic volume; HR, heart rate; LVM, left ventricular mass; S1P<sub>1</sub>, sphingosine-1-phosphate receptor 1; SV, stroke volume.

generated mice deficient for S1P<sub>1</sub> specifically in cardiomyocytes (S1P<sub>1</sub><sup>αMHCcre</sup>). S1P<sub>1</sub><sup>αMHCcre</sup> mice were born with the expected mendelian frequency and appeared indistinguishable from their controls (S1P<sub>1</sub><sup>flox/flox</sup> littermates) at birth; however, S1P<sub>1</sub><sup>αMHCcre</sup> mice began to die prematurely from 34 weeks on, with a median survival time of 45 weeks

(Figure 1A). On autopsy, spontaneously deceased mice presented with enlargement of all cardiac chambers (Figure 1B). Cardiac echocardiography (Figure 1C) at 34 and 48 weeks and magnetic resonance imaging (Figure 1D) in S1P<sub>1</sub><sup>αMHCcre</sup> mice aged 48 weeks revealed clearly impaired LV function compared with controls, as demonstrated by increased end-

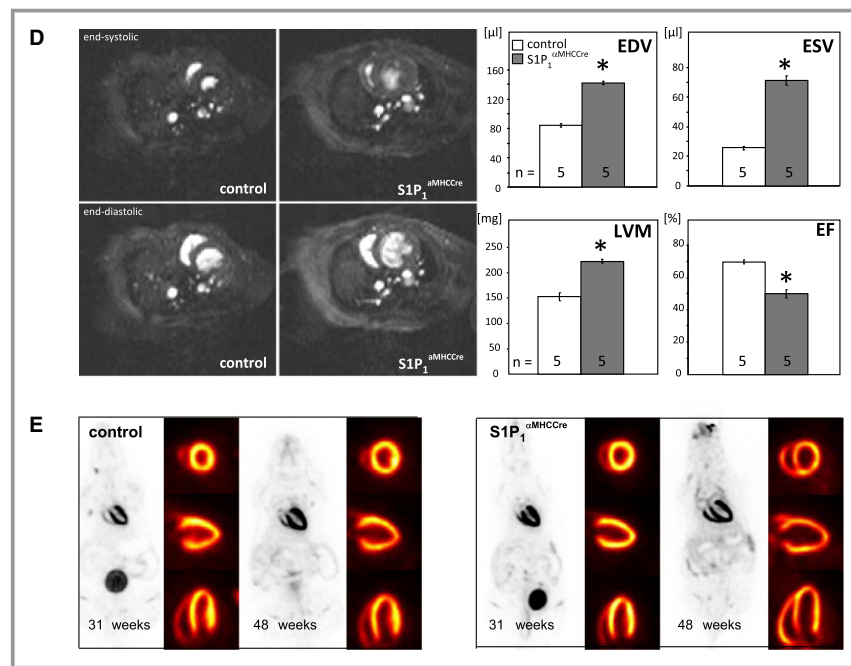


**Figure 1.** Continued.

diastolic and end-systolic volumes, increased LV mass, and reduced ejection fraction and stroke volume. Serial <sup>18</sup>F-fluorodeoxyglucose positron emission tomography imaging excluded myocardial viability defects as a cause of impaired function (Figure 1E). Histomorphometry of the left ventricle revealed cardiac fibrosis in S1P<sub>1</sub><sup>αMHCcre</sup> mice that increased with age but no alterations in cardiomyocyte size (Figure 2A). LV gene expression was altered in S1P<sub>1</sub><sup>αMHCcre</sup> mice: Expression of atrial natriuretic peptide and β-myosin heavy chain was increased ≈6-fold, expression of brain natriuretic peptide was increased 2-fold, and expression of modulatory calcineurin inhibitory protein 1 was increased ≈5-fold compared with controls (Figure 2B).

Invasive cardiac catheterization was then performed to assess LV function in response to adrenergic stimulation in S1P<sub>1</sub><sup>αMHCcre</sup> and control mice aged 38 to 40 weeks (Figure 2C). Maximal rates of contraction and relaxation were reduced with increasing doses of dobutamine in S1P<sub>1</sub><sup>αMHCcre</sup> mice, whereas heart rates and maximal LV pressure were similar to controls (Figure 2C). Similar observations were made in 19–26 weeks old mice (Figure S1).

### Reduced Ca<sup>2+</sup><sub>i</sub> Concentration, Increased Ca<sup>2+</sup><sub>i</sub> Sensitivity, and Attenuated Sarcomere Relaxation in S1P<sub>1</sub><sup>αMHCcre</sup> Cardiomyocytes

To explore the role of S1P<sub>1</sub> at the single-cell level, APs, Ca<sup>2+</sup><sub>i</sub> transients, and sarcomere shortening were examined in single cardiomyocytes from S1P<sub>1</sub><sup>αMHCcre</sup> mice and littermate

controls. APs elicited at 1 to 8 Hz were significantly prolonged in S1P<sub>1</sub><sup>αMHCcre</sup> cardiomyocytes (to 140% for AP duration at 90% repolarization), whereas all other AP parameters were unchanged (Figure 3A). Furthermore, a substantial decrease in diastolic and systolic Ca<sup>2+</sup><sub>i</sub> was observed in S1P<sub>1</sub><sup>αMHCcre</sup> cardiomyocytes compared with controls, whereas Ca<sup>2+</sup><sub>i</sub> transient amplitude remained unchanged (Figure 3B). Time to peak (between 4 and 8 Hz) and time to 80% Ca<sup>2+</sup><sub>i</sub> transient decay (at 4–6 Hz) were delayed (data not shown). Ca<sup>2+</sup> concentration released following caffeine application was clearly reduced in S1P<sub>1</sub><sup>αMHCcre</sup> cardiomyocytes, indicating reduced sarcoplasmic reticulum content (Figure 3C). Basal cAMP levels were increased in S1P<sub>1</sub><sup>αMHCcre</sup> cardiomyocytes (Figure 3D), in agreement with the coupling of S1P<sub>1</sub> to G<sub>i</sub> and its inhibitory effect on adenylate cyclase. Despite the lower absolute Ca<sup>2+</sup><sub>i</sub> values, no changes in diastolic or systolic sarcomere length (SL) or SL amplitude were observed in S1P<sub>1</sub><sup>αMHCcre</sup> cardiomyocytes (Figure 3E); however, the rate of SL shortening was reduced, and the shortening durations increased (time to 90% relaxation at 2 Hz in controls 103±4 versus 120±5 ms in S1P<sub>1</sub><sup>αMHCcre</sup>).

To test whether the preserved contractility of S1P<sub>1</sub><sup>αMHCcre</sup> cardiomyocytes, despite their lower Ca<sup>2+</sup><sub>i</sub>, was caused by increased Ca<sup>2+</sup> responsiveness of the contractile apparatus, we examined Ca<sup>2+</sup> sensitivity in single skinned cardiomyocytes. Indeed, the Ca<sup>2+</sup> sensitivity of force development was clearly increased in skinned S1P<sub>1</sub><sup>αMHCcre</sup> cardiomyocytes compared with controls (Figure 4A). Furthermore, the phosphorylation status of

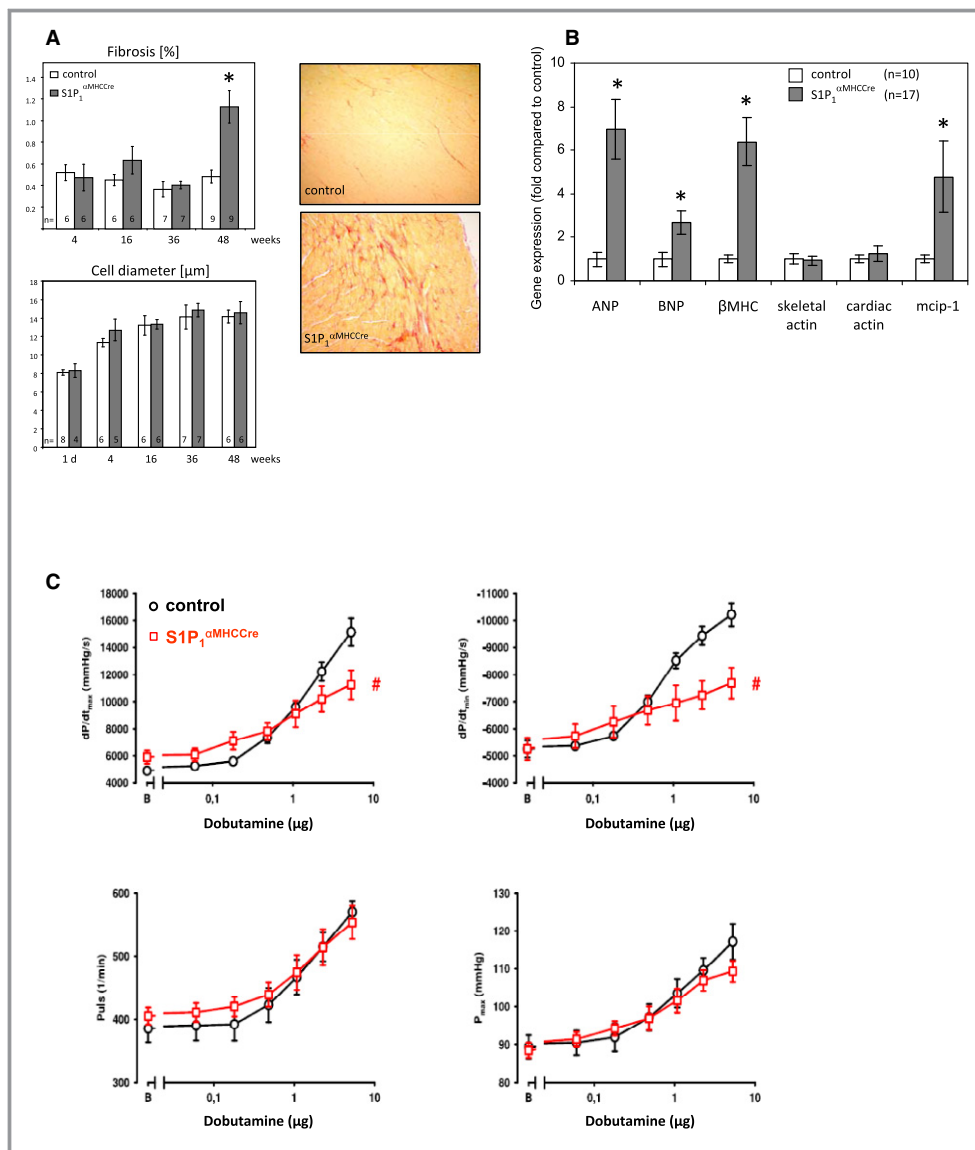


**Figure 2.** Structural and biochemical changes. A, Cardiomyocyte diameters and cardiac fibrosis in S1P<sub>1</sub><sup>αMHCcre</sup> and control hearts at different ages (1 day to 48 weeks). Inset shows representative picosirius red staining of an S1P<sub>1</sub><sup>αMHCcre</sup> mouse heart aged 11 months and its littermate control. B, Gene expression in total heart tissue from S1P<sub>1</sub><sup>αMHCcre</sup> and controls as determined by real-time polymerase chain reaction and expressed relative to control in mice aged 45 to 48 weeks. \*Statistical significance ( $P < 0.05$ ). C, Assessment of left ventricular function in S1P<sub>1</sub><sup>αMHCcre</sup> mice and controls by left ventricular catheterization in S1P<sub>1</sub><sup>αMHCcre</sup> mice aged 38 to 40 weeks ( $n = 7$ ) and their controls ( $n = 7$ ). Maximal rates of contraction and relaxation as well as heart rate and maximal left ventricular pressure were obtained from continuous recordings of left ventricular pressure and volume at basal state B and during continuous infusion of increasing doses of dobutamine. Values are mean  $\pm$  SEM. #Significant ( $P < 0.05$ , 2-way repeated-measures ANOVA) difference in the obtained dobutamine response. ANP indicates atrial natriuretic peptide;  $\beta\text{MHC}$ ,  $\beta$ -myosin heavy chain; BNP, brain natriuretic peptide; dP/dt<sub>max</sub>, maximal rate of contraction; dP/dt<sub>min</sub>, maximal rate of relaxation; mcip-1, modulatory calcineurin inhibitory protein 1; P<sub>max</sub>, maximal left ventricular pressure; S1P<sub>1</sub>, sphingosine-1-phosphate receptor 1.

regulatory myofilament proteins such as myosin light chain 2 and myosin binding protein C was clearly reduced and that of troponin I showed a similar trend (Figure 4B).

Protein levels of sarcoplasmic reticulum Ca<sup>2+</sup> ATPase 2a, junctin, and total and phosphorylated phospholamban were not altered (Table S1).

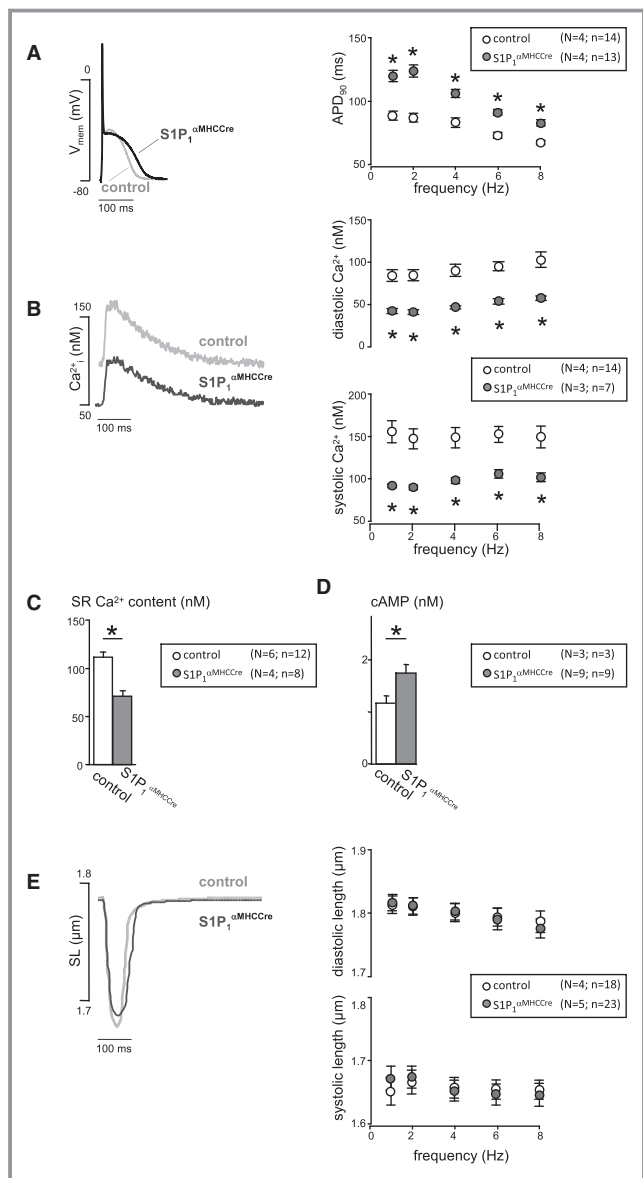


**Figure 3.** Action potentials, Ca<sup>2+</sup> transients, and contractility. Excitation contraction coupling parameters (action potentials, Ca<sup>2+</sup>, transients, and SL shortening) were studied in isolated cardiomyocytes from S1P<sub>1</sub><sup>αMHCCre</sup> mice aged 45 to 48 weeks and control mice. A, Typical action potential traces obtained at 2 Hz (left) and averaged APD<sub>90</sub> recorded at 1 to 8 Hz (right). B, Representative Ca<sup>2+</sup><sub>i</sub> transients obtained at 2 Hz and averaged Ca<sup>2+</sup><sub>i</sub> transient parameters obtained at 1 to 8 Hz. C, Ca<sup>2+</sup> content of the SR (averaged SR Ca<sup>2+</sup> content of cardiomyocytes after 120 seconds of electrical pacing at 6 Hz). D, Cyclic AMP levels. E, Typical traces of SL shortening obtained at 2 Hz (left) and averaged SL parameters measured at 1 to 8 Hz (right). “N” represents the number of animals used for isolation of cardiomyocytes, and “n” indicates the number of total observations in single cardiomyocytes. \*Statistical significance ( $P < 0.05$ ). APD<sub>90</sub> indicates AP duration at 90% repolarization; Ca<sup>2+</sup><sub>i</sub>, intracellular Ca<sup>2+</sup> concentration; S1P<sub>1</sub>, sphingosine-1-phosphate receptor 1; SL, sarcomere length; SR, sarcoplasmic reticulum.

## Decreased Activity of the Na<sup>+</sup>/H<sup>+</sup> Exchanger NHE-1 in S1P<sub>1</sub><sup>αMHCCre</sup> Cardiomyocytes

We next addressed the mechanism behind the low Ca<sup>2+</sup><sub>i</sub> concentrations of S1P<sub>1</sub><sup>αMHCCre</sup> cardiomyocytes. Considering the tight coupling of Ca<sup>2+</sup><sub>i</sub> and Na<sup>+</sup><sub>i</sub> through the Na<sup>+</sup>/Ca<sup>2+</sup> exchanger, we hypothesized that reduced Ca<sup>2+</sup><sub>i</sub> was associated with reduced intracellular Na<sup>+</sup> concentration (Na<sup>+</sup><sub>i</sub>). Indeed, S1P<sub>1</sub><sup>αMHCCre</sup> cardiomyocytes exhibited 23% lower Na<sup>+</sup><sub>i</sub> at all stimulation frequencies (1–8 Hz) (Figure 5A), leading us to test whether reduced Ca<sup>2+</sup><sub>i</sub> might be secondary to lower Na<sup>+</sup><sub>i</sub>. The sarcolemmal NHE-1 and the Na<sup>+</sup> channel are the 2 major routes for Na<sup>+</sup> entry into cardiomyocytes, and because the upstroke velocity of the AP was unchanged, we did not expect alterations in Na<sup>+</sup> channel activity. In contrast, the proton flux through NHE-1 as a measure of NHE-1 activity was dramatically decreased in S1P<sub>1</sub><sup>αMHCCre</sup> cardiomyocytes (Figure 5B). NHE-1 expression was not altered (Figure 5B, inset). This suggested that Na<sup>+</sup> entry through NHE-1 was compromised in the absence of S1P<sub>1</sub>, leading to reduced Ca<sup>2+</sup><sub>i</sub>.

## Pharmacological S1P<sub>1</sub> Inhibition and Blockade of S1P Production Both Diminish Na<sup>+</sup><sub>i</sub> and Ca<sup>2+</sup><sub>i</sub> by Inhibiting NHE-1

To test whether the low NHE-1 activity of S1P<sub>1</sub><sup>αMHCCre</sup> cardiomyocytes could be simulated in control cardiomyocytes, we examined NHE-1 activity in the presence of the S1P<sub>1</sub> antagonist W146.<sup>22</sup> Furthermore, to test if endogenously produced S1P could be activating S1P<sub>1</sub> signaling to control NHE-1 activity, we inhibited sphingosine kinase activity with dimethylsphingosine.<sup>23</sup> Treatment with either W146 or dimethylsphingosine reduced systolic Ca<sup>2+</sup><sub>i</sub>, diastolic Ca<sup>2+</sup><sub>i</sub>, sarcoplasmic reticulum Ca<sup>2+</sup> content, and Na<sup>+</sup><sub>i</sub> down to values as low as those observed in S1P<sub>1</sub><sup>αMHCCre</sup> cardiomyocytes (Figure 5C, 5D and 5E). Consecutive treatment with the NHE-1 inhibitor cariporide did not diminish Na<sup>+</sup><sub>i</sub> any further (Figure 5F and 5G), suggesting that the effect was due to suppression of NHE-1 activity. Nevertheless, this experiment does not exclude the possibility of a “floor effect” below a certain Na<sup>+</sup><sub>i</sub> level. Neither dimethylsphingosine nor W146 affected SL shortening (Figure 5H), completely resembling the phenotype of S1P<sub>1</sub><sup>αMHCCre</sup> cardiomyocytes.

We then addressed whether stimulation with S1P affects contractile function in S1P<sub>1</sub><sup>αMHCCre</sup> cardiomyocytes in the absence and presence of noradrenaline. In the absence of noradrenaline, S1P had no effect on SL in both control and S1P<sub>1</sub><sup>αMHCCre</sup> cardiomyocytes (Figure 5I). In the presence of noradrenaline, S1P decreased SL amplitude and shortened time to 50% relaxation in control cardiomyocytes but failed to do so in S1P<sub>1</sub><sup>αMHCCre</sup> cardiomyocytes (Figure 5J). Furthermore,

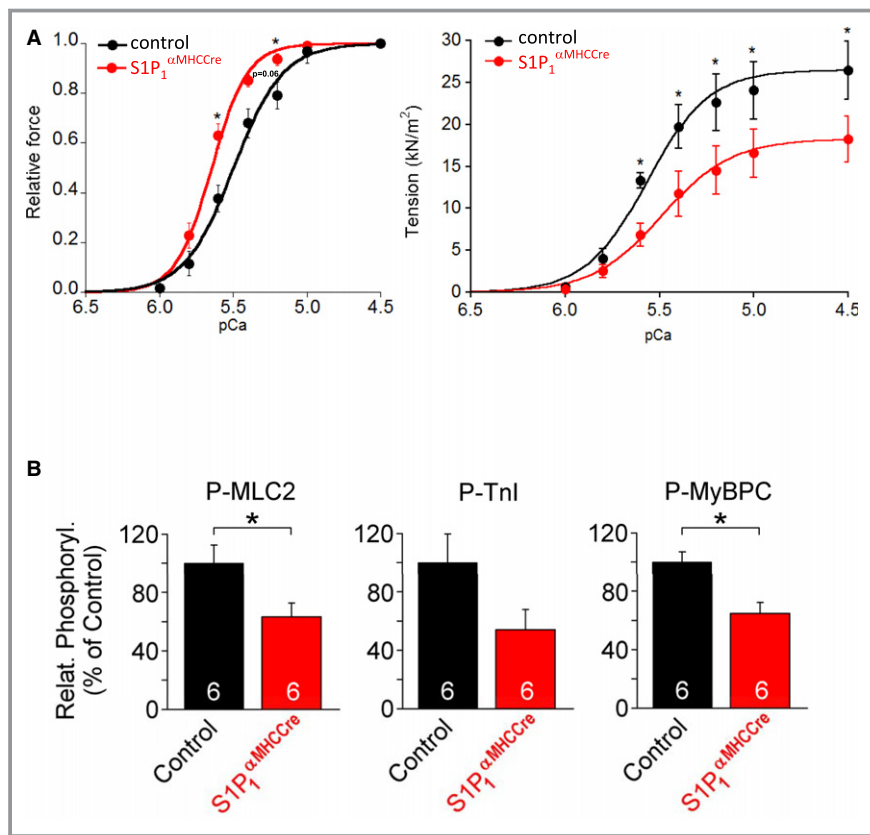


**Figure 4.** Ca<sup>2+</sup> sensitivity of force development and phosphorylation of regulatory myofilament proteins. A, Relative force vs pCa relationship at 2.2- $\mu$ m SL of skinned cardiomyocytes from S1P<sub>1</sub> <sup>$\alpha$ MHCCre</sup> and control mice (10 myocytes per group from 2 mice aged 26 weeks and 2 mice aged 47 weeks that displayed the same phenotype independent of age). Curves are Hill fits to the mean data points. B, Phosphorylation levels of the cardiac myofilament proteins MLC2, Tnl and MyBPC in S1P<sub>1</sub> <sup>$\alpha$ MHCCre</sup> hearts relative to controls. Data are mean $\pm$ SEM for 6 hearts per group (3 mice aged 20 weeks and 3 mice aged 45 weeks that displayed the same phenotype independent of age). MLC2 indicates myosin light chain 2; MyBPC, myosin-binding protein C; P, phosphorylated; pCa,  $-\log$  of [Ca<sup>2+</sup>]; Relat. Phosphoryl., Relative phosphorylation; S1P<sub>1</sub>, sphingosine-1-phosphate receptor 1; Tnl, troponin I.

S1P inhibited noradrenaline-mediated cAMP generation in control but not in S1P<sub>1</sub> <sup>$\alpha$ MHCCre</sup> cardiomyocytes (Figure 5K). Consequently, exogenous S1P exerted an indirect negative inotropic effect through S1P<sub>1</sub> in line with this hallmark feature of G<sub>i</sub>-coupled receptors. These data are in agreement with previous studies showing attenuation of isoproterenol-induced cardiomyocyte contractility by S1P through adenylate cyclase inhibition and its reversal by pharmacological S1P<sub>1</sub> inhibition.<sup>24,25</sup> In summary, S1P<sub>1</sub> activation by acute S1P stimulation reduced  $\beta$ -adrenergic contractility through adenylate cyclase inhibition, whereas continuous S1P<sub>1</sub> signaling by endogenous S1P was required for the maintenance of NHE-1 activity.

### Loss of IP in S1P<sub>1</sub> <sup>$\alpha$ MHCCre</sup> Mice

Several studies have shown that cardiac S1P produced endogenously by sphingosine kinases mediates the

cardioprotective effect of IP<sup>8</sup>; however, the responsible S1P receptor has remained unknown. To test whether S1P<sub>1</sub> was involved, we compared the response to IP in S1P<sub>1</sub> <sup>$\alpha$ MHCCre</sup> and control mice. As expected, IP conferred cardioprotection in controls, but the cardioprotective effect was completely absent in S1P<sub>1</sub> <sup>$\alpha$ MHCCre</sup> mice (Figure 6A). Infarct size without IP was similar in both groups (Figure 6A). The survival kinase Akt is known to be instrumental for the effectiveness of IP in rodents (see review 26). Interestingly, sphingosine kinase 1-deficient mice (Sphk1<sup>-/-</sup>) cannot be preconditioned and cannot activate Akt following IP.<sup>23</sup> Consequently, we examined Akt signaling during IP in S1P<sub>1</sub> <sup>$\alpha$ MHCCre</sup> and control mice and observed that Akt phosphorylation was clearly impaired in IP samples from S1P<sub>1</sub> <sup>$\alpha$ MHCCre</sup> mice compared with controls (Figure 6B). In contrast, there was no difference in basal Akt phosphorylation in noninjured hearts (Figure S2). These data support



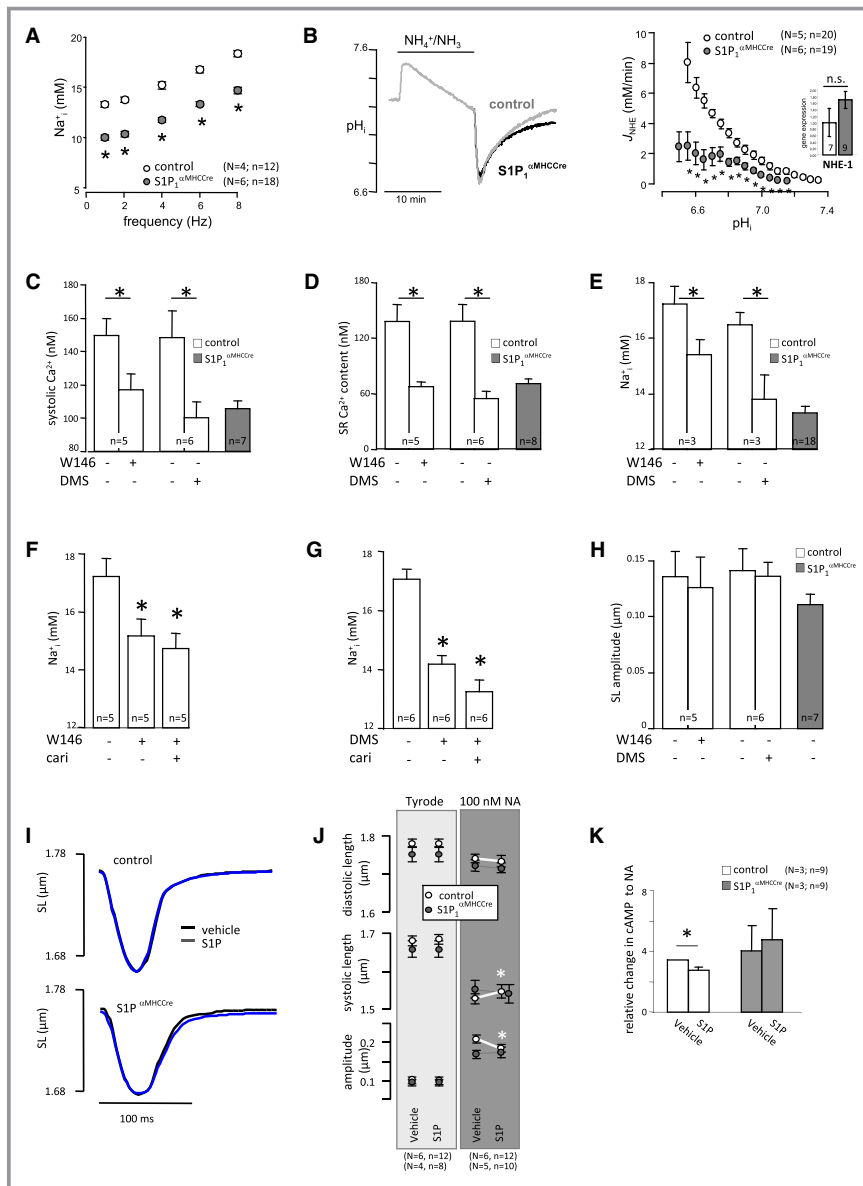


**Figure 5.** Role of S1P<sub>1</sub> in the regulation of NHE-1. A, Na<sup>+</sup><sub>i</sub> concentrations in control and S1P<sub>1</sub><sup>αMHCcre</sup> cardiomyocytes obtained at 1 to 8 Hz. B, NHE-1 activity shown as representative pH<sub>i</sub> traces of acid-load recoveries (left) and averaged pH<sub>i</sub>/J<sub>NHE-1</sub> profiles (right). Inset shows NHE-1 gene expression. C, Systolic Ca<sup>2+</sup><sub>i</sub>, (D) sarcoplasmic reticulum Ca<sup>2+</sup> content, and (E) Na<sup>+</sup><sub>i</sub> in control cardiomyocytes with and without preincubation with W146 (1 μmol/L) and DMS (5 μmol/L), respectively, for 30 minutes. Values for S1P<sub>1</sub><sup>αMHCcre</sup> cardiomyocytes are shown for comparison. F and G, No further reduction of Na<sup>+</sup><sub>i</sub> by cariporide (10 μmol/L) beyond that caused by DMS or W146. H, No effect of W146 and DMS on SL. I and J, SL shortening in the presence of exogenous S1P (100 nmol/L) under basal conditions and after stimulation with NA (100 nmol/L) with electrical pacing of 6 Hz. K, Cyclic AMP levels after NA stimulation without and with exogenous S1P (100 nmol/L) expressed as relative to basal in S1P<sub>1</sub><sup>αMHCcre</sup> cardiomyocytes and their controls. All mice were aged 45 to 48 weeks. “N” represents the number of animals used for isolation of cardiomyocytes and “n” indicates the number of total observations in single cardiomyocytes. \*Statistical significance to vehicle or controls, respectively (P<0.05). DMS, dimethylsphingosine; J<sub>NHE-1</sub>, NHE-1–dependent proton flux; NA, noradrenaline; Na<sup>+</sup><sub>i</sub>, intracellular Na<sup>+</sup> concentration; n.s., not significant; pH<sub>i</sub>, intracellular pH concentration; S1P<sub>1</sub>, sphingosine-1-phosphate receptor 1; SL, sarcomere length.

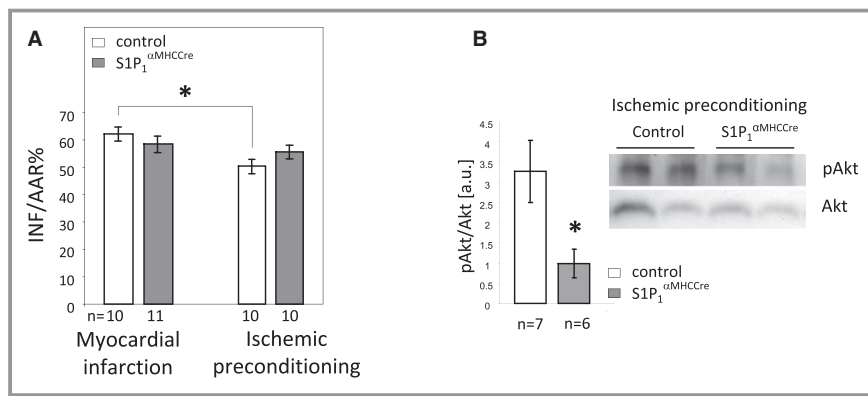


**Figure 6.** Myocardial infarction and ischemic preconditioning in S1P<sub>1</sub><sup>αMHCcre</sup> mice. A, Infarct size/area at risk (INF/AAR) in S1P<sub>1</sub><sup>αMHCcre</sup> and control mice that underwent 30 minutes of coronary occlusion followed by 120 minutes of reperfusion without or with ischemic preconditioning (1 cycle of 5 minutes of occlusion and 10 minutes of reperfusion before occlusion). All mice were aged 18 to 20 weeks. \*Statistical significance ( $P < 0.05$ ) between groups (2-way repeated measures ANOVA followed by Bonferroni). B, Akt phosphorylation (Ser473) in ischemic preconditioning samples of control and S1P<sub>1</sub><sup>αMHCcre</sup> mice at the time of sacrifice after ischemia–reperfusion. S1P<sub>1</sub> indicates sphingosine-1-phosphate receptor 1.

the notion that S1P<sub>1</sub> is responsible for IP and exerts its cardioprotective effect through Akt.

## Discussion

In our study, we identified that continuous S1P<sub>1</sub> signaling is necessary for the maintenance of NHE-1 activity and for dampening of the Ca<sup>2+</sup> sensitivity of the contractile apparatus. The decrease in myofilament contractility caused by S1P<sub>1</sub> signaling most likely takes place through inhibition of adenylate cyclase, consistent with the ability of S1P<sub>1</sub> to inhibit cAMP formation through G<sub>i</sub>. This is conceptually supported by the validity of the reverse because activation of the adenylate cyclase pathway is well known to cause the Ca<sup>2+</sup>-sensitizing effect of many agents such as endothelin 1, noradrenaline, and levosimendan.<sup>27</sup> The functional correlates of this finding were the shortened diastolic and systolic SLs, the reduced rate of SL shortening, and the increased shortening durations in S1P<sub>1</sub><sup>αMHCcre</sup> cardiomyocytes. Its biochemical manifestation was the reduced phosphorylation of myosin light chain 2, myosin binding protein C, and troponin I, which are all substrates for cAMP-activated protein kinase A. The source of S1P to continuously engage S1P<sub>1</sub> was of cardiomyocyte origin and was generated by sphingosine kinases (with the cautionary note that sphingosine kinase inhibition data with dimethylsphingosine should be confirmed by genetic evidence). In this scenario, the lower Ca<sup>2+</sup><sub>i</sub> due to reduced NHE-1 activity in the absence of S1P<sub>1</sub> may serve to balance elevated Ca<sup>2+</sup> sensitivity. Conversely, any reduction in NHE-1 activity and thus of Ca<sup>2+</sup><sub>i</sub> (eg, by decreased endogenous S1P production and thus lower S1P<sub>1</sub> signaling) may be balanced by the

simultaneous increase in Ca<sup>2+</sup> sensitivity. In clear support, transgenic overexpression of NHE-1 has been shown to increase systolic and diastolic Ca<sup>2+</sup><sub>i</sub> without changes in contractility, and lower Ca<sup>2+</sup> sensitivity has been identified as the underlying cause.<sup>28</sup> Although not shown directly in our study, the increase of cAMP in S1P<sub>1</sub><sup>αMHCcre</sup> cardiomyocytes may be suppressing NHE-1 activity because cAMP is a well-known inhibitor of NHE-1.<sup>29,30</sup> In addition, S1P has been shown to stimulate Na<sup>+</sup>/H<sup>+</sup> exchange in thyroid cells.<sup>31</sup> Nevertheless, complex compensatory changes in response to S1P<sub>1</sub> deficiency during development should also be considered. A possible explanation (that needs experimental confirmation) of

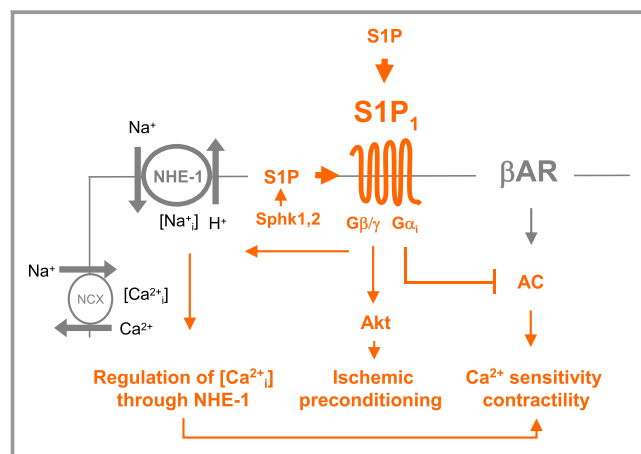


**Figure 7.** Schematic of the role of S1P<sub>1</sub> in the heart. β1-AR indicates β1-adrenoreceptor; NCX, Na<sup>+</sup>/Ca<sup>2+</sup> exchanger; NHE-1, Na<sup>+</sup>/H<sup>+</sup> exchanger; S1P, sphingosine-1-phosphate; S1P<sub>1</sub>, sphingosine-1-phosphate receptor 1; Sphk1, sphingosine kinase 1; Sphk2, sphingosine kinase 2.

how this regulatory system may contribute to cardiac physiology is its potential ability to accommodate hemodynamic challenge by increasing Ca<sup>2+</sup> sensitivity through a reduction of endogenous S1P production and thus S1P<sub>1</sub> signaling; at the same time, lower S1P<sub>1</sub> signaling would suppress NHE-1 activity, thereby reducing Na<sup>+</sup><sub>i</sub> and Ca<sup>2+</sup><sub>i</sub> and providing an elegant in-built safe-guarding mechanism against excessive Ca<sup>2+</sup> sensitization (Figure 7).

IP relies on endogenous S1P synthesis by sphingosine kinases (see review 8), but the S1P receptor mediating IP was unknown. In this study, we identified S1P<sub>1</sub> as the S1P receptor required for the cardioprotective effect of IP. In contrast, S1P<sub>1</sub> played no role in the susceptibility of the heart to regular ischemia–reperfusion injury without IP. The exact mechanisms by which S1P<sub>1</sub> mediates IP are unknown but should be sought in the signaling pathways common to S1P<sub>1</sub> and IP. S1P produced by sphingosine kinases is increased during and indispensable for IP<sup>8</sup> and acts by activating the reperfusion injury salvage kinase pathway and the survivor activating factor enhancement pathway and by decreasing the cardiomyocyte susceptibility to mitochondrial permeability transition pore opening (see review 26). The inability of S1P<sub>1</sub><sup>αMHC<sup>Cre</sup></sup> mice to benefit from IP and their defective Akt activation during preconditioning are consistent with the lack of IP in Sphk1<sup>−/−</sup> mice and their inability to activate the Akt pathway.<sup>2,3</sup> Therefore, S1P<sub>1</sub>/Akt signaling is essential for IP in mice (Figure 7).

A recent study showed that cardiac S1P<sub>1</sub> was downregulated in isoproterenol-induced heart failure in rats and that its overexpression alleviated heart failure after myocardial infarction; the authors suggested downregulation of the β<sub>1</sub>-adrenoreceptor by its cointernalization with S1P<sub>1</sub> as possible cause.<sup>32</sup> We did not see any enhanced contractile response to β-adrenergic stimulation in S1P<sub>1</sub><sup>αMHC<sup>Cre</sup></sup>, as one might expect if there were a pool of β<sub>1</sub>-adrenoreceptors constantly being cointernalized because of constitutive S1P<sub>1</sub> activity—a pool that should be available in surplus for signaling in its absence. In fact, the response of S1P<sub>1</sub><sup>αMHC<sup>Cre</sup></sup> to β-adrenergic stimulation was even worse in vivo and unaffected in vitro. In support, 3 studies showed that long-term FTY70 treatment of mice (a regimen that is generally known to downregulate S1P<sub>1</sub>) improved LV function and survival after myocardial infarction in mice and pigs.<sup>33–35</sup> According to our observations, downregulation of cardiomyocyte S1P<sub>1</sub> may have a beneficial role in heart failure because it would alleviate the compromised Ca<sup>2+</sup> sensitivity of the failing heart and lessen its Ca<sup>2+</sup> overload by subduing the pathologically elevated NHE-1 activity. Future studies in experimental models of heart failure are needed to address these questions. Clearly, the role of S1P and its receptors in cardiac function under physiological and pathophysiological conditions is an exciting new area of research that promises novel ramifications for cardiovascular medicine.

## Acknowledgments

We thankfully acknowledge the excellent technical assistance of K. Abouhamed, D. Reinhard and A. Büchert.

## Sources of Funding

This work was supported by the Deutsche Forschungsgemeinschaft (LE940/3-1, LE940/4-1, Sonderforschungsbereich 656, Münster, projects A6 and Z2 and the Interdisciplinary Centre for Clinical Research, Münster (core unit PIX and Technology & Methods Service CarCeF).

## Disclosures

None.

## References

- Sattler KJ, Elbasan S, Keul P, Elter-Schulz M, Bode C, Graler MH, Brocker-Preuss M, Budde T, Erbel R, Heusch G, Levkau B. Sphingosine 1-phosphate levels in plasma and HDL are altered in coronary artery disease. *Basic Res Cardiol*. 2010;105:821–832.
- Argraves KM, Sethi AA, Gazzolo PJ, Wilkerson BA, Remaley AT, Tybjaerg-Hansen A, Nordestgaard BG, Yeatts SD, Nicholas KS, Barth JL, Argraves WS. S1P, dihydro-S1P and C24:1-ceramide levels in the HDL-containing fraction of serum inversely correlate with occurrence of ischemic heart disease. *Lipids Health Dis*. 2011;10:70.
- Sattler K, Lehmann I, Graler M, Brocker-Preuss M, Erbel R, Heusch G, Levkau B. HDL-bound sphingosine 1-phosphate (S1P) predicts the severity of coronary artery atherosclerosis. *Cell Physiol Biochem*. 2014;34:172–184.
- Egom EE, Mamas MA, Chacko S, Stringer SE, Charlton-Menys V, El-Omar M, Chirico D, Clarke B, Neyses L, Cruickshank JK, Lei M, Fath-Ordoubadi F. Serum sphingolipids level as a novel potential marker for early detection of human myocardial ischaemic injury. *Front Physiol*. 2013;4:130.
- Jing XD, Wei XM, Deng SB, Du JL, Liu YJ, She Q. The relationship between the high-density lipoprotein (HDL)-associated sphingosine-1-phosphate (S1P) and coronary in-stent restenosis. *Clin Chim Acta*. 2015;446:248–252.
- Levkau B. HDL-S1P: cardiovascular functions, disease-associated alterations, and therapeutic applications. *Front Pharmacol*. 2015;6:243.
- Sattler K, Graler M, Keul P, Weske S, Reimann CM, Jindrova H, Kleinbongard P, Sabbadini R, Brocker-Preuss M, Erbel R, Heusch G, Levkau B. Defects of high-density lipoproteins in coronary artery disease caused by low sphingosine-1-phosphate content: correction by sphingosine-1-phosphate-loading. *J Am Coll Cardiol*. 2015;66:1470–1485.
- Karlner JS. Sphingosine kinase and sphingosine 1-phosphate in cardioprotection. *J Cardiovasc Pharmacol*. 2009;53:189–197.
- Means CK, Brown JH. Sphingosine-1-phosphate receptor signalling in the heart. *Cardiovasc Res*. 2009;82:193–200.
- Levkau B. Cardiovascular effects of sphingosine-1-phosphate (S1P). *Handb Exp Pharmacol*. 2013;216:147–170.
- Vessey DA, Li L, Honbo N, Karlner JS. Sphingosine 1-phosphate is an important endogenous cardioprotectant released by ischemic pre- and postconditioning. *Am J Physiol Heart Circ Physiol*. 2009;297:H1429–H1435.
- Theilmeier G, Schmidt C, Herrmann J, Keul P, Schafers M, Herrgott I, Mersmann J, Larmann J, Hermann S, Stypmann J, Schober O, Hildebrand R, Schulz R, Heusch G, Haude M, von Wnuck Lipinski K, Herzog C, Schmitz M, Erbel R, Chun J, Levkau B. High-density lipoproteins and their constituent, sphingosine-1-phosphate, directly protect the heart against ischemia/reperfusion injury in vivo via the S1P<sub>3</sub> lysophospholipid receptor. *Circulation*. 2006;114:1403–1409.
- Means CK, Xiao CY, Li Z, Zhang T, Omens JH, Ishii I, Chun J, Brown JH. Sphingosine 1-phosphate S1P<sub>2</sub> and S1P<sub>3</sub> receptor-mediated Akt activation protects against in vivo myocardial ischemia-reperfusion injury. *Am J Physiol Heart Circ Physiol*. 2007;292:H2944–H2951.
- Sanna MG, Liao J, Jo E, Alfonso C, Ahn MY, Peterson MS, Webb B, Lefebvre S, Chun J, Gray N, Rosen H. Sphingosine 1-phosphate (S1P) receptor subtypes

- S1P1 and S1P3, respectively, regulate lymphocyte recirculation and heart rate. *J Biol Chem*. 2004;279:13839–13848.
15. Luke MM, O'Meara ES, Rowland CM, Shiffman D, Bare LA, Arellano AR, Longstreth WT Jr, Lumley T, Rice K, Tracy RP, Devlin JJ, Psaty BM. Gene variants associated with ischemic stroke: the Cardiovascular Health Study. *Stroke*. 2009;40:363–368.
  16. Shiffman D, O'Meara ES, Bare LA, Rowland CM, Louie JZ, Arellano AR, Lumley T, Rice K, Jakoubova O, Luke MM, Young BA, Malloy MJ, Kane JP, Ellis SG, Tracy RP, Devlin JJ, Psaty BM. Association of gene variants with incident myocardial infarction in the Cardiovascular Health Study. *Arterioscler Thromb Vasc Biol*. 2008;28:173–179.
  17. Choi JW, Gardell SE, Herr DR, Rivera R, Lee CW, Noguchi K, Teo ST, Yung YC, Lu M, Kennedy G, Chun J. FTY720 (fingolimod) efficacy in an animal model of multiple sclerosis requires astrocyte sphingosine 1-phosphate receptor 1 (S1P1) modulation. *Proc Natl Acad Sci USA*. 2010;108:751–756.
  18. Agah R, Frenkel PA, French BA, Michael LH, Overbeek PA, Schneider MD. Gene recombination in postmitotic cells. Targeted expression of Cre recombinase provokes cardiac-restricted, site-specific rearrangement in adult ventricular muscle in vivo. *J Clin Invest*. 1997;100:169–179.
  19. Levkau B, Schafers M, Wohlschlaeger J, von Wnuck Lipinski K, Keul P, Hermann S, Kawaguchi N, Kirchhof P, Fabritz L, Stypmann J, Stegger L, Flogel U, Schrader J, Fischer JW, Hsieh P, Ou YL, Mehrhof F, Tiemann K, Ghanem A, Matus M, Neumann J, Heusch G, Schmid KW, Conway EM, Baba HA. Survivin determines cardiac function by controlling total cardiomyocyte number. *Circulation*. 2008;117:1583–1593.
  20. Hamdani N, Bishu KG, von Frieling-Salewsky M, Redfield MM, Linke WA. Deranged myofilament phosphorylation and function in experimental heart failure with preserved ejection fraction. *Cardiovasc Res*. 2012;97:464–471.
  21. Schwanke U, Konietzka I, Duschin A, Li X, Schulz R, Heusch G. No ischemic preconditioning in heterozygous connexin43-deficient mice. *Am J Physiol Heart Circ Physiol*. 2002;283:H1740–H1742.
  22. Sanna MG, Wang SK, Gonzalez-Cabrera PJ, Don A, Marsolais D, Matheu MP, Wei SH, Parker I, Jo E, Cheng WC, Cahalan MD, Wong CH, Rosen H. Enhancement of capillary leakage and restoration of lymphocyte egress by a chiral S1P1 antagonist in vivo. *Nat Chem Biol*. 2006;2:434–441.
  23. Jin ZQ, Goetzl EJ, Karliner JS. Sphingosine kinase activation mediates ischemic preconditioning in murine heart. *Circulation*. 2004;110:1980–1989.
  24. Means CK, Miyamoto S, Chun J, Brown JH. S1P1 receptor localization confers selectivity for Gi-mediated cAMP and contractile responses. *J Biol Chem*. 2008;283:11954–11963.
  25. Landeen LK, Dederko DA, Kondo CS, Hu BS, Aroonsakool N, Haga JH, Giles WR. Mechanisms of the negative inotropic effects of sphingosine-1-phosphate on adult mouse ventricular myocytes. *Am J Physiol Heart Circ Physiol*. 2008;294:H736–H749.
  26. Heusch G. Molecular basis of cardioprotection: signal transduction in ischemic pre-, post-, and remote conditioning. *Circ Res*. 2015;116:674–699.
  27. Endoh M. Signal transduction and Ca<sup>2+</sup> signaling in intact myocardium. *J Pharmacol Sci*. 2006;100:525–537.
  28. Nakamura TY, Iwata Y, Arai Y, Komamura K, Wakabayashi S. Activation of Na<sup>+</sup>/H<sup>+</sup> exchanger 1 is sufficient to generate Ca<sup>2+</sup> signals that induce cardiac hypertrophy and heart failure. *Circ Res*. 2008;103:891–899.
  29. Vaughan-Jones RD, Swietach P. Pushing and pulling the cardiac sodium/hydrogen exchanger. *Circ Res*. 2008;103:773–775.
  30. Wakabayashi S, Shigekawa M, Pouyssegur J. Molecular physiology of vertebrate Na<sup>+</sup>/H<sup>+</sup> exchangers. *Physiol Rev*. 1997;77:51–74.
  31. Tornquist K. Sphingosine 1-phosphate stimulates Na<sup>+</sup>/H<sup>+</sup> exchange in thyroid FRTL-5 cells. *Am J Physiol*. 1997;272:C1052–C1057.
  32. Cannavo A, Rengo G, Liccardo D, Pagano G, Zincarelli C, De Angelis MC, Puglia R, Di Pietro E, Rabinowitz JE, Barone MV, Cirillo P, Trimarco B, Palmer TM, Ferrara N, Koch WJ, Leosco D, Rapacciuolo A. Beta1-adrenergic receptor and sphingosine-1-phosphate receptor 1 (S1P1) reciprocal downregulation influences cardiac hypertrophic response and progression to heart failure: protective role of S1P1 cardiac gene therapy. *Circulation*. 2013;128:1612–1622.
  33. Wang G, Kim RY, Imhof I, Honbo N, Luk FS, Li K, Kumar N, Zhu BQ, Eberle D, Ching D, Karliner JS, Raffai RL. The immunosuppressant FTY720 prolongs survival in a mouse model of diet-induced coronary atherosclerosis and myocardial infarction. *J Cardiovasc Pharmacol*. 2014;63:132–143.
  34. Luk FS, Kim RY, Li K, Ching D, Wong DK, Joshi SK, Imhof I, Honbo N, Hoover H, Zhu BQ, Lovett DH, Karliner JS, Raffai RL. Immunosuppression with FTY720 reverses cardiac dysfunction in hypomorphic ApoE mice deficient in SR-BI expression that survive myocardial infarction caused by coronary atherosclerosis. *J Cardiovasc Pharmacol*. 2016;67:47–56.
  35. Santos-Gallego CG, Vahl TP, Goliash G, Picatoste B, Arias T, Ishikawa K, Njerve IU, Sanz J, Narula J, Sengupta PP, Hajjar RJ, Fuster V, Badimon JJ. Sphingosine-1-phosphate receptor agonist fingolimod increases myocardial salvage and decreases adverse postinfarction left ventricular remodeling in a porcine model of ischemia/reperfusion. *Circulation*. 2016;133:954–966.

## Supplemental Material

### Methods

#### Functional Characterization of Isolated Cardiomyocytes (Detailed Methods)

Left ventricular myocytes were isolated from adult mice (aged 30-38 weeks) by enzymatic dissociation. Cell size and membrane capacitance of the isolated cardiomyocytes were similar in all genotypes (data not shown). The following parameters were measured as described before<sup>1,2</sup> and detailed here again. Action potential recordings: Action potentials (APs) were recorded using the perforated patch-clamp technique using an Axopatch 200B amplifier (Molecular Devices, Union City, CA). Tyrode's solution ( $36\pm 0.2^\circ\text{C}$ ) contained (in mM): 140 NaCl, 5.4 KCl, 1.8  $\text{CaCl}_2$ , 1  $\text{MgCl}_2$ , 5.5 glucose, 5 HEPES; pH 7.4 (NaOH). Patch pipettes ( $\sim 2.0\ \text{M}\Omega$ ) contained (in mM): 125 K-gluc, 20 KCl, 10 NaCl, 0.22 amphotericin-B, 10 HEPES; pH 7.2 (KOH). APs were filtered and digitized at 10 and 40 kHz, respectively. Custom-made software was used for data acquisition and analysis; potentials were corrected for the calculated liquid junction potential (15 mV). APs were elicited at 1 to 10-Hz by 3-ms,  $\approx 1.2\times$ threshold current pulses through the patch pipette. Resting membrane potential (RMP), maximal AP amplitude (APA), maximal upstroke velocity ( $dV/dt_{\text{max}}$ ), AP duration at 20, 50, and 90% repolarization ( $\text{APD}_{20}$ ,  $\text{APD}_{50}$ , and  $\text{APD}_{90}$ , respectively), and plateau amplitude ( $\text{Pl}_a$ ; defined as the potential difference between RMP and the potential 20-ms after the upstroke) were analyzed and averaged from 10 consecutive APs.  $\text{Ca}^{2+}_i$ ,  $\text{Na}^+_i$  and  $\text{pH}_i$  measurements:  $\text{Ca}^{2+}_i$ ,  $\text{Na}^+_i$  and  $\text{pH}_i$  were measured in indo-1, SBFI, and SNARF-1 loaded myocytes, preincubated in HEPES-buffered solutions containing 10  $\mu\text{M}$  SBFI-AM or 5  $\mu\text{M}$  indo<sub>1</sub>AM or 10  $\mu\text{M}$  SNARF<sub>1</sub>AM and 0.01% pluronic. Incubation durations were 10, 30 and 120 min. Myocytes were washed twice before use with fresh HEPES solution (without albumin) and kept for 15

min to ensure complete deesterification. Excitation wavelengths were 340, 340, and 515 nm, respectively. Fluorescence of all indicators was measured in dual wavelength emission mode at 405/505, 410/590 and 580/640 nm. Fluorescence signals were corrected for background recorded from probe-free myocytes and calibrated to obtain maximum and minimum ratio values of the emitted wavelengths and the constants  $\beta$  and  $k_d$  as described previously<sup>1</sup>.  $Na^+_i$  and  $Ca^{2+}_i$  were calculated with the formulation of Grynkiewicz et al.  $Na^+_i$  was averaged over the entire cardiac cycle because it does not vary on a beat to beat basis. Cytosolic free  $Ca^{2+}_i$  was obtained by correction of measured overall cellular fluorescence signals for contributions of mitochondrially compartmentalized indo-1.  $pH_i$  was determined from calibration curves obtained with nigericin, and NHE-1 dependent proton flux ( $J_{NHE-1}$ ) was calculated from the rate of recovery of  $pH_i$  following acid loading as described in detail in the supplement. The SR  $Ca^{2+}$  content of cells was studied by 20 mM caffeine application. Sarcomere length shortening: Sarcomere length was measured using a fast Fourier transform algorithm of the video image (200 frames/s) of the contracting myocytes (IonOptix, Milton, MA). cAMP measurements: The LANCE cAMP kit (PerkinElmer, Zaventem, Belgium) was used to determine cAMP concentrations (according to the manufacturer's instruction) using a Victor plate reader (Wallac, PerkinElmer, Zaventem, Belgium). Cell suspension was added to a 96-well OptiPlate (PerkinElmer, Waltham, MA, USA; 5  $\mu$ l per well) and incubated for 10 min at 37 °C with vehicle (0.4% albumin), cariporide (10  $\mu$ M), S1P (100 nM) or S1P (100 nM) + cariporide (10  $\mu$ M) either in the absence or in the presence of noradrenaline (100 nM). All experiments were performed in the presence of 0.05% bovine serum albumin (BSA) and 500  $\mu$ M of the phosphodiesterase inhibitor isobutyl-methyl-xanthine (IBMX) to allow accumulation of cAMP. The obtained cAMP values were normalized to the control cAMP value measured in the absence of noradrenaline.

### **pH<sub>i</sub> Fluorescence Measurements in Myocytes**

All procedures have been performed as described previously<sup>2</sup>. In brief, wells of a 96 well plate were initially filled with 200  $\mu$ l Tyrode's solution containing either 0, 1.25, 12.5, 37.5, 125, 375 nmol/l S1P (dissolved in BSA), 0, 1.25, 12.5, 37.5, 125, 375 nmol/l SEW (dissolved in DMSO), or 0, 1.25, 12.5, 37.5, 125, 375 nmol/l FTY720-P (dissolved in BSA) and stored at 37°C until use. The pH<sub>i</sub>-  $J_{\text{NHE-1}}$  flux profile obtained at 0 nM S1P, FTY720-P and SEW2817 contained the same vehicle concentration, (BSA, BSA and DMSO) as used at 300 nM S1P, FTY720-P and SEW2817. Each plate contained also wells filled with 200  $\mu$ l "high K<sup>+</sup>-nigericin" solutions set at different pH values (5.0, 6.0, 6.5, 7.0, 7.5, 8.0 and 9.0) for calibration. Rod-shaped cardiomyocytes were exposed for 30 minutes to 10  $\mu$ mol/l BCECF-AM (dissolved in DMSO). Excess BCECF-AM was removed by centrifugation (300 G for 2 minutes) and supernatant was removed. To acid-load the cardiomyocytes, the pellet was first resuspended in 20 mM NH<sub>4</sub>Cl containing Tyrode's solutions (37°C) and after 15 minutes NH<sub>4</sub>Cl was replaced (300 G for 2 minutes) by 5 ml Na<sup>+</sup>-free Tyrode's solution(37°C). In the absence of Na<sup>+</sup>, cardiomyocytes are unable to recover from the acid-load. To all wells of the 96-well plate, except for the blanco wells, 50  $\mu$ l cell suspension (Na<sup>+</sup>-free Tyrode's solution) was rapidly added with a multichannel pipette. To the wells that serve as blanco controls 50  $\mu$ l cell suspension of cardiomyocytes were added that were not loaded with BCECF. Addition of 50  $\mu$ l Tyrode's solution diluted the S1P, SEW and FTY720-P concentrations to 0, 1.0, 10, 30, 100, 300 nmol/l. The 96 well plate was quickly placed in a plate reader (Novostar) that measured pH fluorescence (excitation 440 and 480 nm; emission at 540 nm) of each well every 20 seconds. During the 30 minutes acid-load recovery temperature was kept at 37°C.  $J_{\text{NHE-1}}$  was calculated as described in the materials and methods section.

## Reagents

Immunological detection of phospholamban (PLB), SERCA2a, calsequestrin and junctin and the fraction of PLB phosphorylated at serine 16 and at threonine 17 were determined as described <sup>3</sup>. We thank Dr. L.R. Jones, Indianapolis, for providing calsequestrin, SERCA2a and junctin antibodies. Other antibodies used for Western blotting were from Santa Cruz Biotechnology (p38, #sc-535) or from Cell Signaling (pERK1/2 (#9101), ERK1/2 (#4695) and pp38 (#9211)).

## Mice

All mice used in the experiments were of similar age and either all male or age and sex-matched. In studies involving age-related phenomena (such as the progressive development of cardiomyopathy), the specific age of the examined mice has been specified in text and figure legend. All animal experiments were in compliance with ethical regulations as approved by the Animal Ethics Committee of the Academic Medical Center, Amsterdam, The Netherlands, and the Landesamt für Natur, Umwelt und Verbraucherschutz (LANUV) Nordrhein-Westfalen, Recklinghausen, Germany, respectively, and are in accordance with EU guidelines (2010/63/EU) on the care and use of laboratory animals.

## Statistics

Overall survival curves were estimated using the Kaplan-Meier method and differences between genotypes were compared by the log-rank test. Average data are presented as mean±SEM in all figures but Fig. 6a where the median (minimum to maximum) has been shown. For all cellular (*in vitro*) and animal (*in vivo*) work, two-sided ANOVA for multiple comparisons (repeated measurements) were used to test whether relationships were significantly different, a two-side paired Student's t-test



was used to test for significant differences within groups (e.g. effect of a drug or echocardiographical measurements in the same animal before and after treatment) and a two-sided unpaired t-test to test for significant difference between two groups, depending on the existence of equal variances and normal distribution of data. Mann-Values of  $P < 0.05$  were considered statistically significant. In all echocardiographical measurements, the investigator was blinded to genotype and treatment. For *in vitro* experiments, sample size has been chosen based on own experience from in previous experiments <sup>4</sup>. For all *in vivo* experiments, sample size was based on established (literature) method-specific sample sizes and our own work on I/R and ischemic preconditioning <sup>4</sup>.

1. Baartscheer, A. et al. Chronic inhibition of Na<sup>+</sup>/H<sup>+</sup>-exchanger attenuates cardiac hypertrophy and prevents cellular remodeling in heart failure. *Cardiovasc Res* 2005; 65: 83-92.
2. van Borren, M.M., Baartscheer, A., Wilders, R. & Ravesloot, J.H. NHE-1 and NBC during pseudo-ischemia/reperfusion in rabbit ventricular myocytes. *J Mol Cell Cardiol* 2004; 37: 567-77.
3. Schwanke, U. et al. No ischemic preconditioning in heterozygous connexin43-deficient mice. *Am J Physiol Heart Circ Physiol* 2002; 283: H1740-2.
4. Matus, M. et al. Cardiomyocyte-specific inactivation of transcription factor CREB in mice. *FASEB J* 2007; 21: 1884-92.

## Supplemental Tables

**Table S1. Expression of Ca<sup>2+</sup>-Regulatory SR Proteins in the Left Ventricle of S1P<sub>1</sub><sup>αMHCCre</sup> Mice and Controls.**

Values are expressed in percent of the mean of the control group. CSQ, calsequestrin; SERCA2a, cardiac isoform of sarcoplasmic Ca<sup>2+</sup>-ATPase; PLN, total phospholamban; S16-PLN, phospholamban phosphorylated at serine 16; T17-PLN, phospholamban phosphorylated at threonine 17; JCN, junctin. \**P* < 0.05 vs. control.

	control (n=10)	S1P <sub>1</sub> <sup>αMHCCre</sup> (n=6)
<b>CSQ</b>	100	90 ± 13
<b>SERCA2a</b>	100	96 ± 4
<b>PLN</b>	100	114 ± 9
<b>S16-PLN</b>	100	98 ± 11
<b>T17-PLN</b>	100	110 ± 6
<b>S16-PLN/PLN</b>	100	90 ± 15
<b>T17-PLN/PLN</b>	100	97 ± 12
<b>PLN/SERCA2a</b>	100	118 ± 6 *

## Supplemental Figures

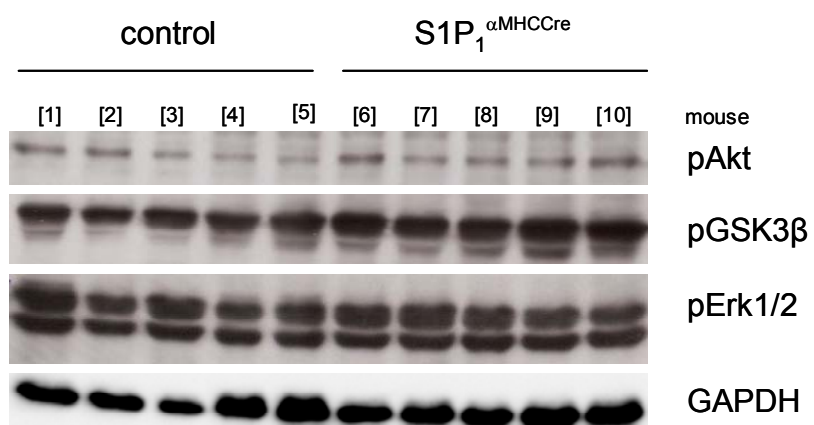


**Figure S1.** Western blotting for phosphorylated (active) kinases in cardiac tissue of control and  $S1P_1^{\alpha MHCcre}$  mice (n=5 each).

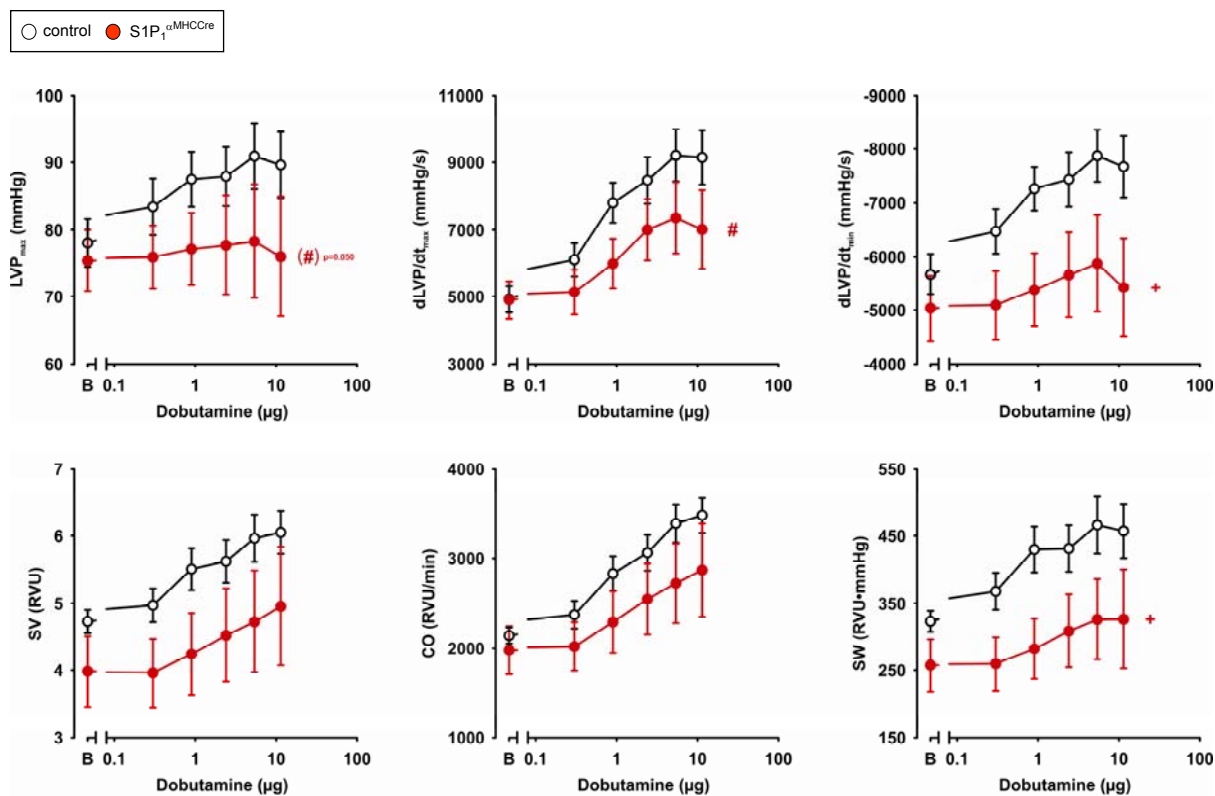


**Figure S2.** Assessment of left-ventricular function in S1P<sub>1</sub><sup>αMHCcre</sup> mice and controls by left ventricular catheterization in 19-26 weeks-old S1P<sub>1</sub><sup>αMHCcre</sup> mice ( $n=7$ ) and controls ( $n=10$ ). Heart rate (HR), left-ventricular pressure (LVP<sub>max</sub>), contraction velocity (dLVP/dt<sub>max</sub>), relaxation velocity (dLVP/dt<sub>min</sub>), stroke volume (SV), cardiac output (CO), and stroke work (SW) were obtained from continuous recordings of left-ventricular pressure and volume at basal state (B) and during continuous infusion of increasing doses of dobutamine. S1P<sub>1</sub><sup>αMHCcre</sup> mice had normal baseline cardiac function but displayed reduced maximal rates of contraction (dLVP/dt<sub>max</sub>), relaxation (dLVP/dt<sub>min</sub>) and stroke work (SW) with increasing doses of dobutamine. Basal and dobutamine-stimulated HR did not differ from controls, while LVP<sub>max</sub> was lower in S1P<sub>1</sub><sup>αMHCcre</sup> mice. Non-floxed mice with and without the Cre transgene were indistinguishable in all parameters excluding Cre effects. Values are mean  $\pm$  SEM. # denotes a significant ( $P < 0.05$ ) difference in the dobutamine response; + denotes a significant ( $P < 0.05$ ) difference in values (2-way repeated measures ANOVA).